Loss of choline agonism in the inner ear hair cell nicotinic acetylcholine receptor linked to the α10 subunit

Marcelo J. Moglie[1†‖], Irina Marcovich[1†§], Jeremías Corradi[2], Agustín E. Carpaneto Freixas[1], Sofía Gallino[1], Paola V. Plazas[3], Cecilia Bouzat[2], Marcela Lipovsek[1,4††], Ana Belén Elgoyhen[1*††]

[1]Instituto de Investigaciones en Ingeniería Genética y Biología Molecular "Dr. Héctor N. Torres" (INGEBI), Consejo Nacional de Investigaciones Científicas y Técnicas (CONICET), Buenos Aires, Argentina

[2]Instituto de Investigaciones Bioquímicas de Bahía Blanca, Departamento de Biología, Bioquímica y Farmacia, Universidad Nacional del Sur y Consejo Nacional de Investigaciones Científicas y Técnicas, Buenos Aires, Argentina.

[3]Instituto de Farmacología, Facultad de Medicina, Universidad de Buenos Aires, Argentina

[4]Centre for Developmental Neurobiology, King's College London, Institute of Psychiatry, Psychology and Neuroscience, Guy's Campus, London, United Kingdom

[‖]Present address: The Francis Crick Institute, London, United Kingdom

[§]Present address: Departments of Otolaryngology & Neurology, Boston Children's Hospital and Harvard Medical School, Boston, MA, USA

[†] These authors equally contributed to this work and share first authorship

[††] These share senior authorship

*Correspondence should be addressed to: Ana Belén Elgoyhen

Instituto de Investigaciones en Ingeniería Genética y Biología Molecular "Dr. Héctor N. Torres" (INGEBI), Consejo Nacional de Investigaciones Científicas y Técnicas (CONICET), Vuelta de Obligado 2490, 1428 Buenos Aires, Argentina.

Phone: +541147832871

Email: elgoyhen@dna.uba.ar

Running Title: Choline efficacy in α9α10 nAChRs

Abstract

The α9α10 nicotinic acetylcholine receptor (nAChR) plays a fundamental role in inner ear physiology. It mediates synaptic transmission between efferent olivocochlear fibers that descend from the brainstem and hair cells of the auditory sensory epithelium. The α9 and α10 subunits have undergone a distinct evolutionary history within the family of nAChRs. Predominantly in mammalian vertebrates, the α9α10 receptor has accumulated changes at the protein level that may ultimately relate to the evolutionary history of the mammalian hearing organ. In the present work we investigated the responses of α9α10 nAChRs to choline, the metabolite of acetylcholine degradation at the synaptic cleft. Whereas choline is a full agonist of chicken α9α10 receptors it is a partial agonist of the rat receptor. Making use of the expression of α9α10 heterologous receptors, encompassing wild-type, heteromeric, homomeric, mutant, chimeric and hybrid receptors, and *in silico* molecular docking, we establish that the mammalian (rat) α10 nAChR subunit underscores the reduced efficacy of choline. Moreover, we show that whereas the complementary face of the α10 subunit does not play an important role in the activation of the receptor by ACh, it is strictly required for choline responses. Thus, we propose that the evolutionary changes acquired in the mammalian α9α10 nAChR resulted in the loss of choline acting as a full agonist at the efferent synapse, without affecting the triggering of ACh responses. This may have accompanied the fine-tuning of hair cell post-synaptic responses to the high frequency activity of efferent medial olivocochlear fibers that modulate the cochlear amplifier.

Keywords: cochlea, nicotinic receptors, evolution, hearing, choline, acetylcholine, ion channels

Contribution to the Field Statement

In the inner ear of mammals, several evolutionary changes have occurred resulting in an expansion of the hearing range to higher sound frequencies. Fine tuning of cochlear synapses is required for sound enconding. The synapse between efferent olivocochlear fibers, that descend from the hindbrain, and sensory hair cells modulates sound amplification at the periphery and it has been proposed as a major player in the expansion of the hearing range. The α9α10 nicotinic acetylcholine receptor, which mediates synaptic neurotransmission at the efferent fiber-hair cell synapses, has accumulated a high number of amino acid substitutions in the mammalian lineage. We now show that these evolutionary acquired changes have led to a mammalian receptor with a lower efficacy for choline, the metabolite produced at the synaptic cleft by acetylcholine degradation. Making use of molecular, electrophysiological and *in silico* simulations techniques we show that it is the α10 subunit the one responsible for the loss of full choline agonism on the efferent receptor in mammals. This functional change may prove fundamental to faithfully reproduce the high frequency activity of efferent medial olivocochlear fibers and the modulation of the cochlear amplifier.

Introduction

The α9α10 nicotinic acetylcholine receptor (nAChR) belongs to the pentameric family of ligand-gated ion channels (Elgoyhen et al., 1994; Elgoyhen et al., 2001; Sgard et al., 2002). Each subunit has a large extracellular N-terminal region, four transmembrane helices (M1–M4), and an intracellular domain. At the interface of the extracellular domains of adjacent subunits lies the orthosteric binding site, composed of a principal component or face provided by one subunit, which contributes three loops of highly conserved residues (loops A–C), and a complementary component of the adjacent subunit, which contributes three loops (loops D–F) with lower levels of sequence conservation among subunits (Thompson et al., 2010). Conserved aromatic residues present within the loops participate in cation-π interactions with the agonists that are fundamental for triggering receptor gating (Karlin, 2002).

The α9α10 receptor is an atypical member of the nAChR family. Both the α9 and α10 subunits have low amino acid sequence identity when compared to other member subunits (Elgoyhen et al., 1994; Elgoyhen et al., 2001; Franchini and Elgoyhen, 2006; Elgoyhen et al., 2009; Lipovsek et al., 2012; Lipovsek et al., 2014; Marcovich et al., 2020) and α9α10 receptors have a baroque pharmacological profile (Rothlin et al., 1999; Verbitsky et al., 2000; Rothlin et al., 2003; Ballestero et al., 2005). Indeed, nicotine, the canonical agonist that characterizes the receptor subfamily, does not activate α9α10 nAChRs, but blocks ACh-gated currents (Elgoyhen et al., 1994; Elgoyhen et al., 2001; Sgard et al., 2002). Moreover, the α9α10 nAChR has a mixed nicotinic and muscarinic profile, since it is blocked by the nicotinic antagonists curare and α-bungarotoxin and the muscarinic antagonist atropine (Elgoyhen et al., 1994; Elgoyhen et al., 2001; Sgard et al., 2002). In addition, the α9α10 receptor shares pharmacological properties with type A γ-aminobutyric acid, glycine, and type 3 serotonin receptors, also members of the pentameric family of ligand-gated ion channels (Rothlin et al., 1999; Rothlin et al., 2003).

The atypical features of the α9α10 receptor prompted the hypothesis that α9 and α10 subunits have undergone a distinct evolutionary history within the family of nAChRs. Using codon-based likelihood models we showed that mammalian, unlike non-mammalian, α10 subunits have been under selective pressure and acquired a greater than expected number of non-synonymous amino acid substitutions in their coding region (Franchini and Elgoyhen, 2006; Elgoyhen and Franchini, 2011). Moreover, mammalian specific amino acid substitutions in the α9 subunit, that show an increased posterior probability of functional divergence in this clade, are involved in the higher relative calcium permeability of mammalian α9α10 receptors (Lipovsek et al., 2014; Marcovich et al., 2020). Overall, these patterns of evolutionary changes at the protein level may relate to the evolutionary history of the mammalian hearing organ (Marcovich et al., 2020), which has the highest frequency sensitivity among vertebrate auditory systems (Manley, 2000). In particular, α9α10 nAChRs mediate the synapses between efferent fibers and sensory hair cells that modulate sound amplification processes, including the mammalian-exclusive prestin-driven somatic electromotility of outer hair cells (OHCs) (Katz and Elgoyhen, 2014; Goutman et al., 2015). Overall, the distinct evolutionary history of mammalian α9α10 nAChRs resulted in differential calcium permeability, current-voltage relationship and desensitization profile of α9α10 receptors

120 across vertebrate species (Lipovsek et al., 2012; Lipovsek et al., 2014; Marcovich et al.,
121 2020), together with the loss of functional homomeric α10 receptors (Elgoyhen et al.,
122 2001; Sgard et al., 2002; Lipovsek et al., 2012) and a non-equivalent contribution of
123 different subunit interfaces to functional binding sites in mammals (Boffi et al., 2017).

124 One striking feature of the pharmacology of mammalian α9α10 receptors, compared to
125 other nAChRs, is the scarcity of identified compounds capable of behaving as agonists
126 of the receptor, since most typical nicotinic agonists block rat α9α10 nAChRs
127 (Verbitsky et al., 2000; Elgoyhen et al., 2001). Whether these observations are related to
128 the peculiar evolutionary history of the mammalian receptor, and do not therefore
129 extend to other non-mammalian α9α10 nAChRs, is still an open question. In the present
130 work we have addressed this by comparing the effects of classical nicotinic agonists:
131 nicotine, carbachol, DMPP and choline, on rat and chicken α9α10 nAChRs. We report
132 that, as for rat receptors, nicotine does not activate but blocks chicken α9α10 nAChRs.
133 However, whereas choline is a partial agonist of rat α9α10 receptors, it is a full agonist
134 of chicken α9α10 receptors. Similarly, DMPP has a higher efficacy in chicken
135 receptors. Using hybrid and chimeric receptors we show that the lower agonistic
136 efficacy of choline in rat α9α10 receptors is linked to the extracellular region of the
137 mammalian α10 subunit. Most importantly, we describe that complementary
138 components of the ligand-binding site provided by the rat α10 subunit non-equivalently
139 contribute to receptor activation by ACh and choline. Thus, whereas ACh does not
140 utilize interfaces where α10 provides the complementary component to elicit maximal
141 responses, choline requires fully competent α10 interfaces for receptor activation,
142 suggesting a requirement for a higher degree of ligand occupancy when choline is the
143 agonist. In line with these results, molecular docking simulations indicate that choline
144 binds at all interfaces with a different orientation with respect to that of ACh, and it
145 does so with differing frequencies depending on which subunit contributes the
146 complementary side. Overall, we propose that the loss of choline full agonism in
147 mammalian α9α10 receptors was driven by changes in the α10 subunit. This may have
148 resulted from functional selection pressure on the fine-tuning of cholinergic responses
149 within the mammalian efferent synapse.

150

151 **Materials and Methods**

152 **Expression of Recombinant Receptors in *X. laevis* oocytes**

153 For expression studies rat and chicken α9 and α10 nAChR subunits subcloned into a
154 modified pGEMHE vector were used. Capped cRNAs were *in vitro* transcribed from
155 linearized plasmid DNA templates using RiboMAX^{TM} Large Scale RNA Production
156 System (Promega, Madison, WI, USA). The maintenance of *X. laevis* and the
157 preparation and cRNA injection of stage V and VI oocytes have been described in detail
158 elsewhere (Verbitsky et al., 2000). Typically, oocytes were injected with 50 nl of
159 RNase-free water containing 0.01 to 1.0 ng of cRNA (at a 1:1 molar ratio for
160 heteromeric receptors) and maintained in Barth's solution (in mM: NaCl 88, $Ca(NO_3)_2$
161 0.33, $CaCl_2$ 0.41, KCl 1, $MgSO_4$ 0.82, $NaHCO_3$ 2.4, HEPES 10) at 18°C.
162 Electrophysiological recordings were performed 2 to 6 days after cRNA injection under
163 two-electrode voltage clamp with an Oocyte Clamp OC-725B or C amplifier (Warner

Instruments Corp., Hamden, CT, USA). Recordings were filtered at a corner frequency of 10 Hz using a 900BT Tunable Active Filter (Frequency Devices Inc., Ottawa, IL, USA). Data acquisition was performed using a Patch Panel PP-50 LAB/1 interphase (Warner Instruments Corp., Hamden, CT, USA) at a rate of 10 points per second. Both voltage and current electrodes were filled with 3 M KCl and had resistances of ~1 MΩ. Data were analyzed using Clampfit from the pClamp 6.1 software. During electrophysiological recordings, oocytes were continuously superfused (~15 ml/min) with normal frog saline composed of: 115 mM NaCl, 2.5 mM KCl, 1.8 mM $CaCl_2$, and 10 mM HEPES buffer, pH 7.2. Drugs were added to the perfusion solution for application. The membrane potential was clamped to -70 mV. To minimize activation of the endogenous Ca^{2+} sensitive chloride current (Elgoyhen et al., 2001), all experiments were performed in oocytes incubated with the Ca^{2+} chelator 1,2-bis (2-aminophenoxy)ethane-N,N,N',N'-tetraacetic acid-acetoxymethyl ester (BAPTA-AM, 100 μM) for 3h before electrophysiological recordings. Concentration-response curves were normalized to the maximal ACh response in each oocyte. For the inhibition curves, nicotine was added to the perfusion solution for 2 min before the addition of 10 μM ACh and then coapplied with this agonist and responses were referred to as a percentage of the response to ACh. The mean and S.E.M. of peak current responses are presented. Agonist concentration-response curves were iteratively fitted, using Prism 6 software (GraphPad Software Inc., La Jolla, CA, USA), with the equation: $I/Imax = A^{nH}/(A^{nH} + EC_{50}^{nH})$, where I is the peak inward current evoked by agonist at concentration A; Imax is the current evoked by the concentration of agonist eliciting a maximal response; EC_{50} is the concentration of agonist inducing half-maximal current response, and nH is the Hill coefficient. An equation of the same form was used to analyze the concentration dependence of antagonist induced blockage. The parameters derived were the concentration of antagonist producing a 50% block of the control response to ACh (IC_{50}) and the associated interaction coefficient (*n*H).

The α10W55T mutant subunit was produced as previously described (Boffi et al., 2017) using Quick change XL II kit (Stratagene, La Jolla, CA, USA). The chimeric α10x construct was generated in two steps. First, the DNA fragment encoding the α10 N-terminal domain was replaced by the DNA sequence encoding the α9 N-terminal domain, by overlap-extension PCR (Horton et al., 1989). Briefly, the DNA sequence of the α9 N-terminal domain was amplified from an α9 pGEMHE construct using primers 5'GGGCGAATTAATTCGAGCTC3' and 5'CACCTTCACTCTCCTTCTGAAGCGCCGCGCTGCAGCCTACGTGTG3', and the DNA sequence of the α10 subunit from TM1 to the C-terminal domain was amplified from an α10 pSGEM construct using primers 5'CACACGTAGGCTGCAGCGCGGCGCTTCAGAAGGAGAGTGAAGGTG3' and 5'GCTATGACCATGATTACGCC3'. The chimeric subunit was amplified using the DNA fragments generated in the two PCRs described above and primers 5'GGGCGAATTAATTCGAGCTC3' and 5'GCTATGACCATGATTACGCC3', and subcloned in pSGEM vector. In a second step, conversion of both the pre TM1 and the TM2-TM3 loop from the chimera to the corresponding α9 sequence was performed by QuikChange Multi Site-Directed Mutagenesis kit (Stratagene) using primers 5'GGCATGCTCTCGGCCACCATCAGCTGGAAGACGG3' and

209 5'GGGCAGCAGGAGGTTGACGATGTAGAATGAAGAGCGGCGCTTCAG3'. All
210 mutant and chimeric subunits were confirmed by sequencing.

211

212 **Recordings from hair cells**

213 Chicken auditory organ (basilar papilla) was dissected from the temporal bone of
214 embryonic chickens (white Leghorns either sex, 17–20 d *in ovo*). The tegmentum
215 vasculosum was removed and the tectorial membrane was stripped from the basilar
216 papilla with most of the short hair cells (SHCs) still attached. This "tectorial
217 preparation" was then inverted and secured in the recording chamber by spring clips.
218 SHCs were recorded in a region 25–50% the distance from the apical (lagenar) to the
219 basal tip of the basilar papilla of the chicken. Apical turns of the organ of Corti were
220 excised from Balb/C mice of either sex between postnatal day 11 (P11) and P13,
221 (around the onset of hearing in altricial rodents). At this age outer hair cells (OHCs) are
222 already innervated by the MOC fibers (Pujol et al., 1998; Simmons, 2002). The tectorial
223 membrane was removed and the organ of Corti was positioned under an insect pin
224 affixed to a cover-slip with a drop of Sylgard.

225 Basilar papilla and cochlear preparations were placed into a chamber on the stage of an
226 upright microscope (Olympus BX51WI, Center Valley, PA, USA) at room temperature
227 and used within 2 h. Cells were visualized on a monitor via a water immersion objective
228 (60× magnification), differential interference contrast optics, and a CCD camera (Andor
229 iXon 885, Belfast, UK). The preparation was superfused continuously at 2–3 mL per
230 min with extracellular saline solution of an ionic composition similar to that of the
231 perilymph: 144 mM NaCl, 5.8 mM KCl, 1.3 mM $CaCl_2$, 0.9 mM $MgCl_2$, 0.7 mM
232 NaH_2PO_4, 5.6 mM D-glucose and 10 mM HEPES buffer (pH 7.4). Solutions containing
233 ACh or choline were prepared in this same saline and delivered by a gravity-fed
234 multichannel glass pipette (150-µm tip diameter).

235 Whole-cell, tight-seal voltage-clamp recordings were made with 1 mm borosilicate
236 glass micropipettes (WPI, Sarasota, FL, USA) ranging from 6 to 8 MΩ tip resistance.
237 Series resistance errors were not compensated for. The recording pipette contained the
238 following (in mM): 140 KCl, 3.5 $MgCl_2$, 2 $CaCl_2$, 5 EGTA, 5 HEPES, 5 mM
239 phosphocreatine-Na_2 and 2.5 Na_2ATP, titrated to pH 7.2 with KOH. Osmolarity was
240 adjusted to 295 mOsM. All recordings were performed at room temperature (22–25 °C).

241 Electrophysiological recordings were performed using a Multiclamp 700B amplifier
242 (Molecular Devices, San Jose, CA, USA), low-pass-filtered at 2–10 kHz, and digitized
243 at 50 kHz via a National Instruments board. Data were acquired using WinWCP (J.
244 Dempster, University of Strathclyde, Glasglow, Scotland). Recordings were analyzed
245 with custom-written routines in IgorPro 6.37 (Wavemetrics, Lake Oswego, OR, USA).

246

247 **Molecular modeling and docking**

248 Homology models of the extracellular domain of the chick and rat α9α10 nAChRs were
249 as in (Boffi et al., 2017). They were created with SWISS MODEL (Schwede et al.,
250 2003; Arnold et al., 2006; Bordoli et al., 2009) using the monomeric structure of the
251 human α9 subunit as the template (Protein Data Bank ID 4UY2;(Zouridakis et al.,

2014)). The monomeric models of these proteins were then structurally aligned to the pentameric structure of *Lymnaea stagnalis* ACh binding protein (AChBP) bound to ACh (Protein Data Bank ID 3WIP; (Olsen et al., 2014)) using the program STAMP (Russell and Barton, 1992) from visual molecular dynamics (Humphrey et al., 1996) to obtain pentameric models with a $(\alpha9)_2(\alpha10)_3$ stoichiometry bound to ACh. Four different types of possible binding site interfaces were included: α9/α9, α9/α10, α10/α9 and α10/α10. For each interface, the first subunit provides the principal face and the second provides the complementary face. The models were energy minimized to relax steric clashes using spdbviewer (Guex and Peitsch, 1997), and were used for docking studies after deletion of ACh from the models. Using Autodock 4.2 (Morris et al., 2009) choline and ACh were downloaded from PubChem and docked into each of the four types of interfaces for rat and chicken subunits. One hundred genetic algorithm runs were performed for each condition. Residues R57, R111, and R117 were set as flexible to avoid steric and/or electrostatic effects that may impair agonist docking into the binding site (Boffi et al., 2017). Clustering of the results was done with Autodock based on a root-mean-square deviation cutoff of 2.0 Å. Docking results were corroborated in three different procedures. The most representative docking result was plotted with Discovery Studio Visualizer 4.5 (Dessault Systèmes BIOVIA, San Diego, 2016).

Statistical Analysis

Statistical analysis was performed using the software Infostat (Universidad Nacional de Córdoba). The non-parametric Mann-Whitney test was used to perform comparisons between two groups and Kruskal-Wallis one-way analysis of variance followed by Conover's test for comparisons between multiple groups. Friedman's test was used for comparisons between paired samples. Differences between samples were considered significant when $p < 0.05$. All raw data and analysis code are available upon request.

Materials

All drugs were obtained from Sigma-Aldrich (St. Louis, MO, USA). ACh, choline, DMPP, carbachol and nicotine were dissolved in distilled water as stocks and stored aliquoted at -20°C. BAPTA-AM was stored at -20°C as aliquots of a 100 mM solution in dimethyl sulfoxide (DMSO), thawed and diluted 1000-fold into Barth's solution shortly before incubation of the oocytes.

All experimental protocols were carried out in accordance with the National Institute of Health Guide for the Care and Use of Laboratory Animals (NIH Publications No. 80-23) revised 1978 and INGEBI Institutional Animal Care and Use Committee.

Results

Cholinergic agonists show lower efficacy on rat α9α10 receptors

The unique pharmacological profile of mammalian α9α10 receptors (Rothlin et al., 1999; Verbitsky et al., 2000; Rothlin et al., 2003), and the observation that mammalian α10 subunits have been under selection pressure (Franchini and Elgoyhen, 2006;

294 Elgoyhen and Franchini, 2011), prompted us to examine whether this baroque
295 pharmacology is recapitulated in receptors from a non-mammalian species. Nicotine,
296 the prototypic agonist of nAChRs, is an antagonist of mammalian α9α10 receptors
297 (Elgoyhen et al., 1994; Elgoyhen et al., 2001; Sgard et al., 2002), and did not elicit
298 currents in oocytes expressing either rat or chicken α9α10 receptors. Instead, nicotine
299 acted as an antagonist of both receptors (Fig. 1A, Table 1 and (Elgoyhen et al., 2001)),
300 blocking responses to 10 μM ACh in a concentration-dependent manner (rat IC_{50} = 46.3
301 ± 12.4 μM; n=6; chicken IC_{50} = 39.4 ± 3.4 μM; n=6; p=0.81, Mann-Whitney test).

302 Next, we analyzed the effect of different nAChR agonists on α9α10 receptors from the
303 two studied species. Previous work showed that ACh elicits maximal responses in both
304 rat and chicken α9α10 receptors, with similar near 10 μM EC_{50} values (Elgoyhen et al.,
305 2001; Lipovsek et al., 2012). The cholinergic agonist carbachol elicited concentration-
306 dependent responses in oocytes expressing α9α10 receptors (Fig. 1B and Table 1) with
307 maximal responses that were 75 ± 5 % (rat, n=5) and 89 ± 7 % (chicken, n=6) of the
308 maximum response elicited by 1 mM ACh (p=0.93, Mann-Whitney test). EC_{50} values
309 for carbachol were similar for the receptors from both species: 159 ± 31.5 μM (rat;
310 n=5), 150 ± 15 μM (chicken; n=6); p=0.42, Mann-Whitney test. The potency of
311 carbachol was therefore nearly 12 times lower compared to that of ACh both in rat and
312 chicken α9α10 recombinant receptors (Elgoyhen et al., 2001; Lipovsek et al., 2012). As
313 previously reported (Elgoyhen et al., 2001), the nicotinic agonist DMPP behaved as a
314 very weak partial agonist of rat α9α10 nAChRs (Fig. 1C and Table 1), with a maximal
315 response that was 0.6 ± 0.3 %, (n=6) of that observed with 1 mM ACh (n=6).
316 Surprisingly, the efficacy of DMPP on chicken α9α10 receptors was significantly higher
317 (p=0.004 Mann-Whitney test compared to rat), reaching 32.6 ± 2.9 % of that of ACh
318 with an EC_{50} of 9.8 ± 0.5 μM (n=5; p=0.03 Mann-Whitney test, chick vs rat). Finally,
319 choline behaved as a partial agonist on rat heteromeric α9α10 receptors (Fig. 1D and
320 Table 1), with a maximal response that was 37 ± 3 % of that produced by 1 mM ACh
321 and an EC_{50} of 541 ± 62 μM (n=10). As observed for DMPP, the efficacy of choline on
322 chicken α9α10 receptors was higher than that observed for rat receptors (n=6; p=0.0004
323 Kruskal-Wallis test), reaching a maximum response of 88 ± 7 % of the maximum
324 response to 1 mM ACh, thus behaving nearly as a full agonist. Additionally, the EC_{50} of
325 200 ± 16 μM (n=6) for choline in chicken α9α10 receptors was nearly three times lower
326 than that observed for rat receptors (EC_{50}= 541 ± 62 (n=10), p=0.0025 Kruskal-Wallis
327 test). In summary, while inhibition by nicotine and agonism by carbachol were similar
328 between chicken and rat receptors, choline and DMPP presented higher efficacies for
329 the avian than for the mammalian α9α10 heteromeric nAChRs.

330

331 **Choline elicits near-maximal responses in chicken, but not in mouse, hair cells**

332 Choline is naturally present at cholinergic synapses as a degradation product of ACh
333 (Wehrwein et al., 2016) and its effect on nAChRs can have important implications for
334 synaptic function (Albuquerque et al., 1998). The synapse between efferent fibers and
335 hair cells is mediated by α9α10 nicotinic receptors coupled to the activation of SK2
336 calcium dependent potassium channels, resulting in an inhibitory response (Fuchs and
337 Murrow, 1992; Dulon and Lenoir, 1996; Katz et al., 2004; Gomez-Casati et al., 2005;
338 Elgoyhen and Katz, 2012). We analyzed the effect of choline in mouse and chicken hair

339 cells in acute explants, in comparison to ACh responses. Figure 2A shows
340 representative responses to both ACh and choline at a holding potential of -40 mV.
341 These responses were outward, resulting from the activation of SK2 potassium channels
342 coupled to the cholinergic responses. For both chicken and mouse hair cells we
343 observed maximal responses to 3 mM ACh. However, and in agreement with that
344 observed for recombinant α9α10 receptors, choline exhibited higher efficacy in chicken
345 hair cells (90 ± 6 %, n=3) when compared to that on mouse hair cells (50 ± 9 %, n=6;
346 p=0.024 Mann-Whitney test). These observations suggest that the differences in
347 agonistic behavior identified in recombinant α9α10 receptors are recapitulated by the
348 native receptors present in chicken and mouse hair cells.

349

350 **The α10 subunit determines choline potency and efficacy in α9α10 nAChRs**

351 In order to determine if the agonistic characteristics of choline could be traced back to
352 the constituent subunits of the α9α10 heteromeric receptors, we first tested the potency
353 of choline on homomeric α9 and α10 nAChRs. Of note, mammalian α10 receptors do
354 not assemble into functional homomeric receptors (Elgoyhen et al., 2001; Sgard et al.,
355 2002) and were therefore not tested.

356 In contrast to that observed for rat heteromeric α9α10 receptors (Fig. 1D), choline
357 behaved as a nearly full agonist of rat α9 receptors (Fig. 3A and Table 1). Thus,
358 although less potent than ACh (EC_{50} choline 188 ± 40, n=3; ACh 12.9 ± 1.1, n=5;
359 p=0.04 Mann-Whitney test), the maximal choline response was 87 ± 6 % (n=4, p=0.002
360 Kruskal-Wallis test) of that elicited by 1 mM ACh. Additionally, the EC_{50} for choline
361 observed for the rat α9 receptor was smaller than that of the rat α9α10 receptor (Fig 1D,
362 p=0.02 Kruskal-Wallis test). It is worth noting that choline was previously shown to be
363 nearly a full agonist of rat α9 homomeric receptors, albeit with a higher potency than
364 that observed here (Verbitsky et al., 2000). Differences might derive from the fact that
365 experiments in the present work were performed in the presence of BAPTA-AM to
366 isolate the cholinergic responses from the secondary activation of the Ca^{2+} sensitive
367 chloride current present in oocytes (Miledi and Parker, 1984), while this was not the
368 case in the previous work (Verbitsky et al., 2000).

369 Choline had high efficacy in both chicken α9 and α10 homomeric receptors, similar to
370 that observed for the chicken α9α10 heteromeric receptor (Table 1). The maximal
371 choline response in chicken α9 receptors was 73.7 ± 5.9 % (n=6) of that obtained for 1
372 mM ACh (Fig. 3B), and it matched the maximal ACh response in chicken α10 receptors
373 (99.4 ± 9.5 % (n=4); Fig. 3C). Choline potency was lower compared to that of ACh for
374 both chicken homomeric receptors and concentration-response curves to choline were
375 shifted to the right with higher EC_{50} values (Fig. 3B-C). For chicken α9, choline showed
376 an EC_{50} = 280 ± 20 μM (n=6) compared to 12.9 ± 1.4 μM for ACh (n=5, p=0.004
377 Mann-Whitney test). In chicken α10 receptors the EC_{50} for choline was 23.2 ± 8.3 μM
378 (n=4), compared to 2.2 ± 0.7 μM for ACh (n=5, p=0.016 Mann-Whitney test).

379 In summary, choline behaved as an agonist with high efficacy for homomeric receptors
380 composed of rat α9, chicken α9 or chicken α10 subunits. This agonistic behavior was
381 similar to that observed for chicken α9α10 receptors but differed from that of rat α9α10
382 heteromeric receptors.

383 The observation that choline behaved as a partial agonist of heteromeric rat α9α10
384 receptors, but a full agonist of rat α9 homomeric nAChRs, suggests that the rat α10
385 subunit may contain determinants responsible for the lower efficacy of choline on
386 heteromeric α9α10 receptors. In order to test this hypothesis, we expressed rat-chicken
387 hybrid receptors in *X. laevis* oocytes (Fig. 4). We previously determined that responses
388 in these hybrid α9α10 receptors are indeed the result of heteromeric assemblies and not
389 individual homomeric receptors (Lipovsek et al., 2014). As shown in Figure 4A, rat α9
390 – chicken α10 hybrid receptors responded to ACh with an EC_{50} of 11.6 ± 2.9 μM (n=7),
391 similar to that of rat (EC_{50} 17.1 ± 3.1 μM, n=5, p=0.19 Kruskal-Wallis test) and chicken
392 (EC_{50} 13.1 ± 2.6 μM, n=10, p=0.67 Kruskal-Wallis test) α9α10 nAChRs (Table 1).
393 Distinct from that described for rat α9α10 receptors (Fig. 1D), choline produced near
394 maximal responses in rat α9 – chicken α10 hybrid receptors (86 ± 2 % of responses to 1
395 mM ACh, n=6), that were similar to those observed in chicken α9α10 receptors (88 ± 7
396 %, n = 6). On the other hand, hybrid chicken α9 – rat α10 receptors exhibited similar
397 concentration-response curves to ACh when compared to rat and chicken α9α10
398 receptors, with an EC_{50} of 18.2 ± 4.8 μM (n=4, p=0.99 and p=0.29, respectively,
399 Kruskal-Wallis test; Fig. 4B and Table 1). However, the maximal response to choline of
400 chicken α9 – rat α10 hybrid receptors (51 ± 6 %, n=5) was smaller than that observed
401 for chicken α9α10 receptors (88 ± 7 %, n=10, p=0.02 Kruskal-Wallis test; Fig. 1C),
402 with a lower efficacy, similar to that of rat α9α10 receptors (37.5 ± 2.5 %, n=9, p=0.50
403 Kruskal-Wallis test).

404 In summary, both the potency and efficacy of choline were lowest for rat heteromeric
405 α9α10 receptors than all other receptors, with the exception of heteromeric hybrid
406 receptors containing rat α10 subunits, therefore suggesting that the rat α10 subunit may
407 hold the molecular determinants of choline's partial agonism (Fig. 4C).

408

409 **Lower frequency of choline binding at orthosteric sites holding rat α10 subunits as**
410 **complementary components**

411 To gain further insight into the mechanism underlying the drop in choline agonism on
412 receptors containing the rat α10 subunit, we performed molecular docking simulations
413 and analyzed the interaction of ACh and choline with the orthosteric binding site. To
414 this end, we used homology models of the extracellular domains of rat and chicken
415 α9α10 receptors with subunit arrangements corresponding to the four possible binding
416 site interfaces (principal/complementary components): α9/α9, α9/α10, α10/α9 and
417 α10/α10 as previously reported (Boffi et al., 2017). We then performed molecular
418 docking analysis of the interaction of ACh or choline with the homology-modeled
419 subunit interfaces to evaluate the orientation, the best binding energy (BBE) and the
420 frequency of conformations that bind the agonist in a favorable orientation within the
421 binding pocket. The conformations considered as favorable were those that showed
422 typical cation-π interactions between the amino group of the ligands and aromatic
423 residues of the binding pocket (W55, from the complementary face, and Y93, W149,
424 Y190 and/or Y197 from the principal face) required for ACh responses (Dougherty,
425 2007; Olsen et al., 2014).

426 As reported previously (Boffi et al., 2017), both for rat and chicken receptors, ACh
427 docking resulted in an energetically favorable model with ACh oriented with its
428 quaternary amine toward the membrane side or lower part of the cleft and the negative
429 charge oriented upwards in the cleft (Fig. 5A and B), similar to ACh in AChBP (Olsen
430 et al., 2014). In this orientation, ACh showed BBE between -3.5 and -6 kcal/mol for the
431 different binding interfaces (Fig. 5E) and its positively charged group showed the
432 potential to form the typical cation-π interactions with the main aromatic residues Y93,
433 W149, Y190, Y197 and W55 (Fig. 5B and C). Thus, as reported for other nAChRs, the
434 orientation of ACh in the binding pocket of rat and chicken α9α10 receptors is favorable
435 for efficacious activation (Fig. 5 and (Boffi et al., 2017)).

436 For all interfaces, choline docked into the orthosteric binding site with two different
437 orientations. The least frequent orientation was similar to that described for choline
438 docked into the muscle nAChR (Bruhova and Auerbach, 2017). In the most frequent
439 and lowest BBE conformation, choline was located more horizontally with respect to
440 the membrane compared to ACh, oriented towards the C-loop containing Y190 and
441 Y197, with the quaternary ammonium placed in the aromatic cavity (Fig. 5B and D).
442 This orientation has also been described for other ligands in different nAChR models
443 (Tomaselli et al., 1991; Lester et al., 2004; Hernando et al., 2012). In this orientation,
444 choline showed the potential to make typical cation-π interactions with the aromatic
445 residues at the principal (W149, Y93, Y190, Y197) and complementary (W55)
446 components (Fig. 5D). Whereas ACh formed an H-bond with the backbone amine
447 group of residue D119 (Boffi, 2017 and Fig. 5B and C), choline formed an H-bond with
448 the carboxyl group of D119 (Fig. 5B and D). Altogether, the orientation and potential
449 interactions with residues indicate that choline adopts a favorable conformation (though
450 different to that of ACh) for eliciting receptor activation, with lower BBEs than those
451 observed for ACh (between -4 and -4.5 kcal/ mol for all interfaces).

452 The orientation and main interactions of choline with residues at the binding site were
453 identical for all interfaces and between chicken and rat receptors. Also, while the BBE
454 for choline did not show significant inter-species differences across the alternate
455 interfaces, we observed variations in the frequency at which choline bound with
456 favorable conformations to the different interfaces (Fig. 5E). Those binding interfaces
457 containing α9 as the complementary subunit (α9/α9 and α10/α9) showed high frequency
458 of choline binding in the favorable conformations both for chicken and rat subunits
459 (Fig. 5E). In contrast, differences were encountered at interfaces in which α10 provided
460 the complementary side (α9/α10 and α10/α10). While each agonist binding frequency
461 for chicken interfaces was similar to that observed with α9 as the complementary
462 subunit, it was significantly lower for interfaces showing a rat α10 complementary
463 subunit (Fig. 5F).

464 Thus, our *in silico* studies focused on the binding site interfaces suggest that the
465 differences of choline responses may be governed by the distinct choline orientation and
466 the differential contribution of binding interfaces containing α10 as the complementary
467 subunit. While in chicken α9α10 receptors a high frequency of choline binding was
468 observed for all conformations of binding sites, in rat α9α10 receptors the frequency of
469 choline binding was significantly lower at α9/α10 and α10/α10 sites, suggesting that the
470 lower choline agonism observed in rat α10 containing receptors (Figures 3 and 4) may

471 be related to a reduced capability of the rat α10 subunit to efficiently operate as the
472 complementary side during agonist binding and receptor gating. Consequently, a
473 reduction in the binding frequency of agonists at specific interfaces might determine
474 differential responses in the context of receptor function.

475

476 **The extracellular region of the rat α10 subunit underpins lower choline efficacy**

477 The N-terminal and TM2-TM3 extracellular domains of nicotinic receptors bare
478 residues involved both in agonist binding and coupling to pore opening (Karlin, 2002;
479 Bouzat et al., 2004), and most likely contain determinants for agonist efficacy (Gupta et
480 al., 2017; Mukhtasimova and Sine, 2018). Given that choline partial agonism was
481 observed when rat α10 subunits are present in the heteromeric receptors (Fig. 4C) and
482 that, although it binds to all binding site combinations, the frequency of favorable
483 choline binding was lower at interfaces in which rat α10 provided the complementary
484 face (Fig. 5F), we hypothesized that a receptor in which no binding site contains α10
485 components would show strong choline agonism. To test this, we engineered a rat α9-
486 α10 ($\alpha10_x$) chimeric subunit in which the entire N-terminal and TM2-TM3 extracellular
487 regions of the rat α10 subunit were replaced by the corresponding domains of the rat α9
488 subunit (Fig. 6A). The chimeric subunit did not form functional homomeric receptors
489 by itself, nor did it do so when co-expressed with the rat α10 subunit. However, when
490 co-expressed with the rat α9 subunit, strong ACh responses were recorded for rat
491 $\alpha9\alpha10_x$ receptors (Fig. 6B), with I_{max} = 269 ± 103 nA (n=5). This contrasts the maximal
492 ACh responses observed for homomeric rat α9 receptors (I_{max} of 14 ± 2 nA, n=4 and see
493 (Elgoyhen et al., 2001), indicating that, when co-expressed, rat α9 and chimeric $\alpha10_x$
494 subunits form heteromeric assemblies. Concentration-response curves for ACh on rat
495 $\alpha9\alpha10_x$ receptors were similar to those of rat α9α10 wild-type receptors with an EC_{50} of
496 15.6 ± 6.5 μM (n=4, p=0.50 Kruskal-Wallis test) (Fig. 6C). Interestingly, responses to
497 choline of the rat $\alpha9\alpha10_x$ chimeric receptor resembled those exhibited by rat α9
498 homomeric receptors and differed from those of rat α9α10 receptors. Thus, the EC_{50} for
499 choline on $\alpha9\alpha10_x$ receptors was 160.2 ± 7.6 μM (n=5), significantly smaller than that
500 in rat α9α10 receptors (541 ± 62 μM, n=10, p=0.007, Kruskal-Wallis test) and similar to
501 that observed in homomeric rat α9 receptors (Fig. 6C and Table 1). Likewise, choline-
502 evoked maximal response of 74 ± 1 % (n=5) in $\alpha9\alpha10_x$ receptors was higher than that of
503 rat α9α10 (38 ± 3 %, n=9, p=0.04 Kruskal-Wallis test) but similar to that observed in rat
504 α9 homomeric receptors (87 ± 6 %, n=4, p=0.27, Kruskal-Wallis test) (Fig. 6C and
505 Table 1). Taken together, the experimental evaluation of ACh and choline agonism in
506 the chimeric receptor indicates that the extracellular region of the rat α10 subunit bears
507 determinants that reduce the efficacy of choline on the α9α10 receptor.

508

509 **The α10 complementary component participates in activation by choline of rat**
510 **α9α10 nAChRs**

511 In a previous work we showed that rat α10 subunits do not contribute with
512 complementary faces to the ACh binding site (Boffi et al., 2017). In contrast, in the
513 present study we have so far shown that the extracellular domain of the rat α10 subunit
514 is responsible for the decrease in choline agonism in rat α9α10 receptors. Moreover, *in*

515 *silico* docking showed that the frequency of choline binding in the correct conformation
516 is lower at interfaces where the complementary component is provided by rat α10
517 subunits (Fig. 5E), suggesting that the lower choline agonism observed in rat α9α10
518 receptors may result from sub-functional α9/α10 or α10/α10 binding sites. Therefore, to
519 evaluate experimentally choline's requirement for functional binding sites containing
520 α10 complementary components, we studied responses to choline on rat α9α10
521 heteromeric receptors holding the W55T mutation in the rat α10 subunits (Fig. 7A).
522 W55 is located within loop D of the complementary component of the binding site,
523 which by directly interacting with the agonist is crucial for binding-gating transduction
524 (Olsen et al., 2014). While responses to ACh showed no significant changes in the
525 α9α10W55T receptor compared to wild type α9α10 receptors (Boffi et al., 2017), Fig.
526 7A and B and Table 1 - EC_{50} α9α10: 17.1 ± 3.1 μM, n=5; EC_{50} α9α10W55T: 37.8 ± 6.2
527 μM, n=8; p=0.06, Kruskal-Wallis test), responses to choline were nearly abolished in
528 mutant receptors. Thus, responses to 10 mM choline were 7 ± 2 % (n=5) of those
529 elicited by 1 mM ACh (Fig. 7B). This indicates that the contribution of the
530 complementary face of the rat α10 subunit to the agonistic effect of ACh and choline is
531 non-equivalent. Thus, whereas rat α10 complementary faces are not required for ACh
532 activation of rat α9α10 receptors (see also (Boffi et al., 2017), intact rat α10
533 complementary components are required for choline agonistic effect.

534 Finally, to evaluate whether choline interacts with the α10/α9 intact interfaces in the
535 α9α10W55T receptor, and therefore also requires them to elicit its reduced agonism, we
536 analyzed responses to 10 μM ACh in the presence of increasing concentrations of
537 choline for both rat α9α10 and α9α10W55T receptors (Fig. 7C and D). ACh was added
538 once a maximal response to choline was observed. The maximal response obtained
539 during the co-application was normalized to the response to 10 μM ACh (Fig. 7C). At
540 low choline concentrations, that do not trigger channel opening (< 100 μM), ACh
541 responses became increasingly smaller as choline concentration increased, both in the
542 α9α10 and the α9α10W55T receptors, suggesting that choline is capable of competing
543 with ACh for the available binding sites. However, in the presence of higher choline
544 concentrations (>300 μM), total responses in α9α10 receptors increased while they
545 remained unchanged for the mutant receptor (Fig. 7D). The V-shaped effect observed in
546 the α9α10 receptor, where an EC_{50} ACh response is blocked at low concentrations of
547 choline and summation of both agonist responses occurs at higher choline
548 concentrations, is consistent with choline acting as a partial agonist (Zhu, 2005) and
549 suggests that the increase in combined response may be due to choline binding to the
550 α9/α10 and α10/α10 sites that are spared by ACh. Conversely, the lack of increase of
551 ACh responses at higher choline concentrations in the α9α10W55T mutant receptor
552 indicates a loss of choline agonism that may result from the unavailability of additional
553 α9/α10 and α10/α10 sites due to the W55T mutation.

554 Overall, the differences observed in the responses to ACh and/or choline between
555 α9α10 wild type and α9α10W55T mutant receptors indicate that the complementary
556 faces of α10 subunits are required for the partial agonistic effect of choline on α9α10
557 receptors, therefore suggesting that choline necessitates higher binding site occupancy
558 compared to ACh to elicit channel gating of rat α9α10 nAChRs.

559

560 **Discussion**

561 The present work shows that the mammalian (rat) α10 nAChR subunit is responsible for
562 a reduced efficacy of choline when assembled into heteromeric α9α10 receptors. Thus,
563 whereas choline is a full agonist of rat α9 homomeric receptors, it is a partial agonist of
564 rat α9α10 nAChRs. This is further supported by hybrid receptors, on which choline is a
565 full agonist of rat α9 – chicken α10 receptors and the efficacy in chicken heteromeric
566 receptors is reduced when the chicken α10 subunit is replaced by the rat α10 subunit in
567 the chicken α9 – rat α10 assembly. The reduced agonist efficacy determined by the rat
568 α10 subunit is probably extended to other compounds that behave as partial agonists, as
569 evidenced in the present work for DMPP. These results add to the differential functional
570 properties between mammalian and non-mammalian vertebrate α9α10 nAChRs that
571 have been shaped by the more prevalent occurrence of non-synonymous amino acid
572 substitutions during the evolution of mammalian subunits (Franchini and Elgoyhen,
573 2006; Elgoyhen and Franchini, 2011; Lipovsek et al., 2012; Lipovsek et al., 2014;
574 Marcovich et al., 2020).

575 Full and partial agonists evoke distinct structural changes in opening the muscle
576 acetylcholine receptor channel (Mukhtasimova and Sine, 2018). This is further
577 supported by the observation that the αE45R mutation within the binding–gating
578 transduction domain of this receptor attenuates channel opening by a full agonist,
579 whereas it enhances channel opening by a partial agonist (Mukhtasimova and Sine,
580 2013). It was therefore suggested that, due to differences in size and/or chemical
581 structure, different agonists of the same receptor might bind in different conformations
582 and/or strength to the ligand interaction pocket (Mukhtasimova and Sine, 2018). This
583 resembles our observations on the effect of mutating W55 in the rat α10 subunit which
584 greatly impairs the response of the α9α10 receptor to choline but not to ACh.

585 This functional non-equivalence between agonists is further supported by docking
586 analysis, which shows that ACh and choline adopt different conformations at the
587 binding site of α9α10 receptors. This result fully agrees with previous studies in the
588 muscle nAChR (Bruhova and Auerbach, 2017), for which choline and ACh sit at
589 different orientations at the binding site. In our model, choline had two probable
590 alternate orientations compared to ACh with the least frequent one resembling the one
591 described for the muscle nAChR (Bruhova and Auerbach, 2017). Furthermore, the non-
592 equivalence of the agonist binding sites for ACh and choline is reflected in differential
593 atomic interactions. Thus, similar to ACh, choline can make interactions at the aromatic
594 cage. However, whereas ACh makes a H-bond with the backbone amine group of D119
595 of the complementary face, choline shows the potential to make a H-bond with the
596 carboxyl group of the same residue (Fig. 5B and D). Similar to that reported for the
597 muscle ACh receptor (Bruhova and Auerbach, 2017), this different orientation leads to
598 the displacement of the quaternary ammonium of choline away from a favorable
599 position in the aromatic cage compared to ACh. This might lead to a weaker interaction
600 with all aromatic rings of the binding site, accounting for the lower apparent affinity of
601 choline compared to ACh for the α9α10 receptor. Moreover, due to the particular
602 orientation of choline towards the C-loop when compared to ACh, differential
603 interactions with residues of the complementary face and/or degree of closure of the C-

604 loop required for channel gating (Thompson et al., 2010), might be involved in the
605 reduced choline efficacy.

606 Our combined *in silico* and experimental observations allow us further insight into the
607 differential responses to ACh and choline of rat α9α10 nAChRs. Whereas the
608 complementary face of the α10 subunit does not play an important role in the activation
609 of the receptor by ACh, it is strictly required for choline responses, as shown by the
610 results of the W55T mutation. ACh adopts a different and more favorable conformation,
611 better placed within the aromatic pocket compared to choline, and would therefore only
612 require occupying two of the five binding sites, sparing binding sites in which the
613 complementary face is provided by the α10 subunit. However, since choline adopts a
614 less favorable conformation, it probably requires higher binding site occupancy for full
615 efficacy. Differences in agonist efficacy according to available binding sites have been
616 reported for other nAChRs. For example, the α4β2 nAChR in the $(\alpha4)_3(\beta2)_2$
617 stoichiometry contains three functional agonist binding sites for ACh (Harpsøe et al.,
618 2011; Mazzaferro et al., 2011), and the engagement of all three agonist sites produces
619 maximal activation. The agonist site at the α4/α4 interface is a key determinant of
620 agonist efficacy as occupancy of this site increases agonist efficacy, whereas exclusion
621 from the site leads to partial agonism (Mazzaferro et al., 2014). Another example is
622 provided by the α7 receptor. Even though maximal activation requires occupancy of
623 three binding sites in the α7-5HT_3A chimera (Rayes et al., 2009), only one is required in
624 the α7 nAChR (Andersen et al., 2013). Thus, the relationship between binding site
625 occupancy and maximal response differs between nAChRs. Moreover, and in light of
626 our results, we propose that the degree of occupancy required for maximal responses
627 varies with the type of agonist.

628 Hair cell α9α10 nAChRs are distinct from other nicotinic receptors in that a greater
629 divergence in their coding sequence has translated into differential functional properties
630 across clades (Lipovsek et al., 2012; Lipovsek et al., 2014; Marcovich et al., 2020). Our
631 observations here that choline, the degradation product of ACh, has differential
632 agonistic effects on rodent vs avian α9α10 receptors, suggests different scenarios for the
633 workings of the respective efferent synapses. Recordings on native cholinergic
634 responses recapitulated our observations in recombinant rat and chick α9α10 receptors.
635 While choline elicited maximal responses in chicken hair cells, it behaved as a partial
636 agonist of the native nicotinic receptors present in hair cells of mice (Fig. 2). These
637 results imply that in chicken efferent synapses to (mostly) short hair cells, the release of
638 ACh from efferent terminals triggers α9α10 receptors that would continue to be
639 activated in response to the choline produced by ACh degradation due to
640 acetylcholinesterase (AChE) activity, until it is removed from the synaptic cleft. This
641 would result in longer post-synaptic responses subjected to large variations and poor
642 temporal tuning (Katz and Miledi, 1973). In contrast, in mammalian efferent
643 olivocochlear synapses, the degradation of ACh to choline would limit the time-course
644 and improve the reliability of the cholinergic response. Given that choline is not able to
645 fully activate the rodent α9α10 receptor, and in the presence of ACh acts as a
646 competitive antagonist, the termination of α9α10 responses would therefore be dictated
647 by the fast kinetics of AChE activity (Hall, 1973). An apical to basal concentration and
648 isoform diversity gradient of AChE has been described in the mouse cochlea

649 (Emmerling and Sobkowicz, 1988). Notably, the high-frequency basal region exhibits
650 higher concentrations of this enzyme and is enriched in isoforms with faster kinetics,
651 underscoring the relevance of fine temporal tuning of efferent modulation for high
652 frequency sound detection (Emmerling and Sobkowicz, 1988). Additionally, BK
653 channels, that display larger currents with faster kinetics than SK2 channels, participate
654 in efferent synaptic inhibition in higher frequency regions of the cochlea, supporting the
655 notion that an accurate control of OHCs membrane potential is required for the
656 amplification and modulation of high frequency hearing (Rohmann et al., 2015).
657 Finally, compared to chicken, the mammalian α9α10 receptor shows greater
658 desensitization to ACh and higher calcium permeability (Lipovsek et al., 2012;
659 Lipovsek et al., 2014; Marcovich et al., 2020). In addition, the postsynaptic space
660 delimited by a closely juxtaposed subsynaptic cistern is more restricted in mammals
661 (Fuchs et al., 2014; Im et al., 2014), which may contribute to elicit highly localized
662 α9α10-dependent rises in calcium concentration uncoupled from internal calcium stores
663 (Moglie et al., 2018; Moglie et al., 2020). Together with the poorer choline agonism,
664 these multiple functional adaptations may have contributed to "tighter" ACh responses,
665 which may prove fundamental to faithfully reproduce the high frequency activity of
666 efferent medial olivocochlear fibers (Ballestero et al., 2011), therefore fine-tuning the
667 modulation of the OHC cochlear amplifier and contributing to the expansion of the
668 mammalian hearing range.

669 The lower agonistic action of choline on mammalian α9α10 receptors is likely due to
670 the accumulation of amino acid changes within the mammalian α10 subunit (Franchini
671 and Elgoyhen, 2006; Lipovsek et al., 2012) that rendered a subfunctional contribution of
672 α10 as a complementary component subunit. Our *in silico* and experimental analysis of
673 choline agonism indicate that, for it to trigger a full response, it needs to bind to α9/α10
674 and/or α10/α10 sites, therefore requiring sites holding α10 complementary interfaces.
675 This is in contrast with the agonism by ACh, that only requires binding to α10/α9 (or
676 α9/α9) sites formed by an α10 (or α9) principal component and α9 complementary
677 component (Boffi et al., 2017). We hypothesize that amino acid changes within the α10
678 subunit that affect agonist binding and/or receptor triggering from the additional binding
679 sites (i.e. those that have an α10 subunit as a complementary component) would not be
680 deleterious and therefore not under negative selection, as they would not affect the main
681 response to ACh, given that the sensitivity for this agonist is the same in the different
682 species (Lipovsek et al., 2012; Marcovich et al., 2020). In this context, a scenario could
683 be proposed in which strong positive selection pressure for the loss of the agonistic
684 function of choline, a likely functional requirement for fine-tuned high-frequency
685 efferent olivocochlear activity, may have been the driver for the accumulation of coding
686 sequence changes within the extracellular domain of mammalian α10 subunits
687 (Franchini and Elgoyhen, 2006). This then resulted in the loss of choline acting as a full
688 agonist for mammalian α9α10 receptors, without affecting the triggering of ACh
689 responses.

690

691 **Acknowledgments:**

692 We thank Paul A. Fuchs for assistance in the performance of chicken hair cell
693 recordings. This work was supported by Agencia Nacional de Promoción Científicas y

Técnicas, Argentina, the Scientific Grand Prize of the Fondation Pour l'Audition, and NIH grant R01 DC001508 (Paul Fuchs PI and ABE co-PI) to A.B.E.

References

Albuquerque, E.X., Pereira, E.F., Braga, M.F., and Alkondon, M. (1998). Contribution of nicotinic receptors to the function of synapses in the central nervous system: the action of choline as a selective agonist of alpha 7 receptors. *J Physiol Paris* 92(3-4)**,** 309-316. doi: 10.1016/s0928-4257(98)80039-9.

Andersen, N., Corradi, J., Sine, S.M., and Bouzat, C. (2013). Stoichiometry for activation of neuronal α7 nicotinic receptors. *Proc Natl Acad Sci U S A* 110(51)**,** 20819-20824. doi: 10.1073/pnas.1315775110.

Arnold, K., Bordoli, L., Kopp, J., and Schwede, T. (2006). The SWISS-MODEL workspace: a web-based environment for protein structure homology modelling. *Bioinformatics* 22(2)**,** 195-201. doi: 10.1093/bioinformatics/bti770.

Ballestero, J., Zorrilla de San Martin, J., Goutman, J., Elgoyhen, A.B., Fuchs, P.A., and Katz, E. (2011). Short-term synaptic plasticity regulates the level of olivocochlear inhibition to auditory hair cells. *J Neurosci* 31(41)**,** 14763-14774. doi: 10.1523/jneurosci.6788-10.2011.

Ballestero, J.A., Plazas, P.V., Kracun, S., Gomez-Casati, M.E., Taranda, J., Rothlin, C.V., et al. (2005). Effects of quinine, quinidine, and chloroquine on alpha9alpha10 nicotinic cholinergic receptors. *Mol Pharmacol* 68(3)**,** 822-829. doi: mol.105.014431 [pii]
10.1124/mol.105.014431 [doi].

Boffi, J.C., Marcovich, I., Gill-Thind, J.K., Corradi, J., Collins, T., Lipovsek, M.M., et al. (2017). Differential Contribution of Subunit Interfaces to alpha9alpha10 Nicotinic Acetylcholine Receptor Function. *Mol Pharmacol* 91(3)**,** 250-262. doi: 10.1124/mol.116.107482.

Bordoli, L., Kiefer, F., Arnold, K., Benkert, P., Battey, J., and Schwede, T. (2009). Protein structure homology modeling using SWISS-MODEL workspace. *Nat Protoc* 4(1)**,** 1-13. doi: 10.1038/nprot.2008.197.

Bouzat, C., Gumilar, F., Spitzmaul, G., Wang, H.L., Rayes, D., Hansen, S.B., et al. (2004). Coupling of agonist binding to channel gating in an ACh-binding protein linked to an ion channel. *Nature* 430(7002)**,** 896-900. doi: 10.1038/nature02753.

Bruhova, I., and Auerbach, A. (2017). Molecular recognition at cholinergic synapses: acetylcholine versus choline. *J Physiol* 595(4)**,** 1253-1261. doi: 10.1113/jp273291.

Dougherty, D.A. (2007). Cation-pi interactions involving aromatic amino acids. *J Nutr* 137(6 Suppl 1)**,** 1504S-1508S; discussion 1516S-1517S. doi: 10.1093/jn/137.6.1504S.

Dulon, D., and Lenoir, M. (1996). Cholinergic responses in developing outer hair cells of the rat cochlea. *European J. Neurosci* 8**,** 1945-1952.

Elgoyhen, A.B., and Franchini, L.F. (2011). Prestin and the cholinergic receptor of hair cells: Positively-selected proteins in mammals. *Hear Res* 273(1-2)**,** 100-108. doi: S0378-5955(09)00328-1 [pii]
10.1016/j.heares.2009.12.028 [doi].

Elgoyhen, A.B., Johnson, D.S., Boulter, J., Vetter, D.E., and Heinemann, S. (1994). a9: an acetylcholine receptor with novel pharmacological properties expressed in rat cochlear hair cells. *Cell* 79**,** 705-715.

742 Elgoyhen, A.B., and Katz, E. (2012). The efferent medial olivocochlear-hair cell
743 synapse. *J Physiol Paris* 106(1-2)**,** 47-56. doi: 10.1016/j.jphysparis.2011.06.001.
744 Elgoyhen, A.B., Katz, E., and Fuchs, P.A. (2009). The nicotinic receptor of cochlear
745 hair cells: a possible pharmacotherapeutic target? *Biochem Pharmacol* 78(7)**,**
746 712-719. doi: S0006-2952(09)00436-5 [pii]
747 10.1016/j.bcp.2009.05.023 [doi].
748 Elgoyhen, A.B., Vetter, D., Katz, E., Rothlin, C., Heinemann, S., and Boulter, J. (2001).
749 Alpha 10: A determinant of nicotinic cholinergic receptor function in
750 mammalian vestibular and cochlear mechanosensory hair cells. *Proc Natl Acad*
751 *Sci USA* 98**,** 3501-3506.
752 Emmerling, M.R., and Sobkowicz, H.M. (1988). Differentiation and distribution of
753 acetylcholinesterase molecular forms in the mouse cochlea. *Hear Res* 32(2-3)**,**
754 137-145. doi: 10.1016/0378-5955(88)90086-x.
755 Franchini, L.F., and Elgoyhen, A.B. (2006). Adaptive evolution in mammalian proteins
756 involved in cochlear outer hair cell electromotility. *Mol Phylogenet Evol* 41(3)**,**
757 622-635. doi: S1055-7903(06)00201-6 [pii]
758 10.1016/j.ympev.2006.05.042 [doi].
759 Fuchs, P.A., Lehar, M., and Hiel, H. (2014). Ultrastructure of cisternal synapses on
760 outer hair cells of the mouse cochlea. *J Comp Neurol* 522(3)**,** 717-729. doi:
761 10.1002/cne.23478.
762 Fuchs, P.A., and Murrow, B.W. (1992). A novel cholinergic receptor mediates
763 inhibition of chick cochlear hair cells. *Proc. R. Soc. Lond. B* 248**,** 35-40.
764 Gomez-Casati, M.E., Fuchs, P.A., Elgoyhen, A.B., and Katz, E. (2005). Biophysical
765 and pharmacological characterization of nicotinic cholinergic receptors in
766 cochlear inner hair cells. *J Physiol* 566**,** 103-118.
767 Goutman, J.D., Elgoyhen, A.B., and Gomez-Casati, M.E. (2015). Cochlear hair cells:
768 The sound-sensing machines. *FEBS Lett* 589(22)**,** 3354-3361. doi:
769 10.1016/j.febslet.2015.08.030.
770 Guex, N., and Peitsch, M.C. (1997). SWISS-MODEL and the Swiss-PdbViewer: an
771 environment for comparative protein modeling. *Electrophoresis* 18(15)**,** 2714-
772 2723. doi: 10.1002/elps.1150181505.
773 Gupta, S., Chakraborty, S., Vij, R., and Auerbach, A. (2017). A mechanism for
774 acetylcholine receptor gating based on structure, coupling, phi, and flip. *J Gen*
775 *Physiol* 149(1)**,** 85-103. doi: 10.1085/jgp.201611673.
776 Hall, Z.W. (1973). Multiple forms of acetylcholinesterase and their distribution in
777 endplate and non-endplate regions of rat diaphragm muscle. *J Neurobiol* 4(4)**,**
778 343-361. doi: 10.1002/neu.480040404.
779 Harpsøe, K., Ahring, P.K., Christensen, J.K., Jensen, M.L., Peters, D., and Balle, T.
780 (2011). Unraveling the high- and low-sensitivity agonist responses of nicotinic
781 acetylcholine receptors. *J Neurosci* 31(30)**,** 10759-10766. doi:
782 10.1523/jneurosci.1509-11.2011.
783 Hernando, G., Bergé, I., Rayes, D., and Bouzat, C. (2012). Contribution of subunits to
784 Caenorhabditis elegans levamisole-sensitive nicotinic receptor function. *Mol*
785 *Pharmacol* 82(3)**,** 550-560. doi: 10.1124/mol.112.079962.
786 Horton, R.M., Hunt, H.D., Ho, S.N., Pullen, J.K., and Pease, L.R. (1989). Engineering
787 hybrid genes without the use of restriction enzymes: gene splicing by overlap
788 extension. *Gene (Amst.)* 77**,** 61-68.
789 Humphrey, W., Dalke, A., and Schulten, K. (1996). VMD: visual molecular dynamics.
790 *J Mol Graph* 14(1)**,** 33-38, 27-38. doi: 10.1016/0263-7855(96)00018-5.

Im, G.J., Moskowitz, H.S., Lehar, M., Hiel, H., and Fuchs, P.A. (2014). Synaptic calcium regulation in hair cells of the chicken basilar papilla. *J Neurosci* 34(50)**,** 16688-16697. doi: 10.1523/jneurosci.2615-14.2014.

Karlin, A. (2002). Ion channel structure: emerging structure of the nicotinic acetylcholine receptors. *Nature Reviews Neurosc* 3**,** 102-114.

Katz, B., and Miledi, R. (1973). The binding of acetylcholine to receptors and its removal from the synaptic cleft. *J Physiol* 231(3)**,** 549-574. doi: 10.1113/jphysiol.1973.sp010248.

Katz, E., and Elgoyhen, A.B. (2014). Short-term plasticity and modulation of synaptic transmission at mammalian inhibitory cholinergic olivocochlear synapses. *Front Syst Neurosci* 8**,** 224. doi: 10.3389/fnsys.2014.00224.

Katz, E., Elgoyhen, A.B., Gomez-Casati, M.E., Knipper, M., Vetter, D.E., Fuchs, P.A., et al. (2004). Developmental regulation of nicotinic synapses on cochlear inner hair cells. *J Neurosci* 24(36)**,** 7814-7820.

Lester, H.A., Dibas, M.I., Dahan, D.S., Leite, J.F., and Dougherty, D.A. (2004). Cys-loop receptors: new twists and turns. *Trends Neurosci* 27(6)**,** 329-336. doi: 10.1016/j.tins.2004.04.002.

Lipovsek, M., Fierro, A., Perez, E.G., Boffi, J.C., Millar, N.S., Fuchs, P.A., et al. (2014). Tracking the molecular evolution of calcium permeability in a nicotinic acetylcholine receptor. *Mol Biol Evol* 31(12)**,** 3250-3265. doi: 10.1093/molbev/msu258.

Lipovsek, M., Im, G.J., Franchini, L.F., Pisciottano, F., Katz, E., Fuchs, P.A., et al. (2012). Phylogenetic differences in calcium permeability of the auditory hair cell cholinergic nicotinic receptor. *Proc Natl Acad Sci U S A* 109(11)**,** 4308-4313. doi: 10.1073/pnas.1115488109.

Manley, G.A. (2000). Cochlear mechanisms from a phylogenetic viewpoint. *Proc Natl Acad Sci U S A* 97(22)**,** 11736-11743.

Marcovich, I., Moglie, M.J., Carpaneto Freixas, A.E., Trigila, A.P., Franchini, L.F., Plazas, P.V., et al. (2020). Distinct Evolutionary Trajectories of Neuronal and Hair Cell Nicotinic Acetylcholine Receptors. *Mol Biol Evol* 37(4)**,** 1070-1089. doi: 10.1093/molbev/msz290.

Mazzaferro, S., Benallegue, N., Carbone, A., Gasparri, F., Vijayan, R., Biggin, P.C., et al. (2011). Additional acetylcholine (ACh) binding site at alpha4/alpha4 interface of (alpha4beta2)2alpha4 nicotinic receptor influences agonist sensitivity. *J Biol Chem* 286(35)**,** 31043-31054. doi: 10.1074/jbc.M111.262014.

Mazzaferro, S., Gasparri, F., New, K., Alcaino, C., Faundez, M., Iturriaga Vasquez, P., et al. (2014). Non-equivalent ligand selectivity of agonist sites in (α4β2)2α4 nicotinic acetylcholine receptors: a key determinant of agonist efficacy. *J Biol Chem* 289(31)**,** 21795-21806. doi: 10.1074/jbc.M114.555136.

Miledi, R., and Parker, I. (1984). Chloride current induced by injection of calcium into Xenopus oocytes. *J. Physiol. (Lond).* 357**,** 173-183.

Moglie, M.J., Fuchs, P.A., Elgoyhen, A.B., and Goutman, J.D. (2018). Compartmentalization of antagonistic Ca(2+) signals in developing cochlear hair cells. *Proc Natl Acad Sci U S A* 115(9)**,** E2095-e2104. doi: 10.1073/pnas.1719077115.

Moglie, M.J., Wengier, D.L., Elgoyhen, A.B., and Goutman, J.D. (2020). Synaptic contributions to cochlear outer hair cell Ca²⁺ homeostasis. *bioRxiv*.

Morris, G.M., Huey, R., Lindstrom, W., Sanner, M.F., Belew, R.K., Goodsell, D.S., et al. (2009). AutoDock4 and AutoDockTools4: Automated docking with selective receptor flexibility. *J Comput Chem* 30(16)**,** 2785-2791. doi: 10.1002/jcc.21256.

841 Mukhtasimova, N., and Sine, S.M. (2013). Nicotinic receptor transduction zone:
842 invariant arginine couples to multiple electron-rich residues. *Biophys J* 104(2)**,**
843 355-367. doi: 10.1016/j.bpj.2012.12.013.
844 Mukhtasimova, N., and Sine, S.M. (2018). Full and partial agonists evoke distinct
845 structural changes in opening the muscle acetylcholine receptor channel. *J Gen*
846 *Physiol* 150(5)**,** 713-729. doi: 10.1085/jgp.201711881.
847 Olsen, J.A., Balle, T., Gajhede, M., Ahring, P.K., and Kastrup, J.S. (2014). Molecular
848 recognition of the neurotransmitter acetylcholine by an acetylcholine binding
849 protein reveals determinants of binding to nicotinic acetylcholine receptors.
850 *PLoS One* 9(3)**,** e91232. doi: 10.1371/journal.pone.0091232.
851 Pujol, R., Lavigne-Revillard, M., and Lenoir, M. (1998). "Development of Sensory and
852 Neural Structures in the Mammalian Cochlea," in *Development of the Auditory*
853 *System,* eds. E. Rubel, A. Popper & R. Fay. (New York: Springer), 146-192.
854 Rayes, D., De Rosa, M.J., Sine, S.M., and Bouzat, C. (2009). Number and locations of
855 agonist binding sites required to activate homomeric Cys-loop receptors. *J*
856 *Neurosci* 29(18)**,** 6022-6032. doi: 10.1523/jneurosci.0627-09.2009.
857 Rohmann, K.N., Wersinger, E., Braude, J.P., Pyott, S.J., and Fuchs, P.A. (2015).
858 Activation of BK and SK channels by efferent synapses on outer hair cells in
859 high-frequency regions of the rodent cochlea. *J Neurosci* 35(5)**,** 1821-1830. doi:
860 10.1523/jneurosci.2790-14.2015.
861 Rothlin, C., Verbitsky, M., Katz, E., and Elgoyhen, A. (1999). The α9 nicotinic
862 acetylcholine receptor shares pharmacological properties with type A γ-
863 aminobutyric acid, glycine and type 3 serotonin receptors. *Molec. Pharmacol.*
864 55**,** 248-254.
865 Rothlin, C.V., Lioudyno, M.I., Silbering, A.F., Plazas, P.V., Casati, M.E., Katz, E., et
866 al. (2003). Direct interaction of serotonin type 3 receptor ligands with
867 recombinant and native alpha 9 alpha 10-containing nicotinic cholinergic
868 receptors. *Mol Pharmacol* 63(5)**,** 1067-1074.
869 Russell, R.B., and Barton, G.J. (1992). Multiple protein sequence alignment from
870 tertiary structure comparison: assignment of global and residue confidence
871 levels. *Proteins* 14(2)**,** 309-323. doi: 10.1002/prot.340140216.
872 Schwede, T., Kopp, J., Guex, N., and Peitsch, M.C. (2003). SWISS-MODEL: An
873 automated protein homology-modeling server. *Nucleic Acids Res* 31(13)**,** 3381-
874 3385. doi: 10.1093/nar/gkg520.
875 Sgard, F., Charpentier, E., Bertrand, S., Walker, N., Caput, D., Graham, D., et al.
876 (2002). A novel human nicotinic receptor subunit, α10, that confers
877 functionality to the α9-subunit. *Molec Pharmacol* 61**,** 150-159.
878 Simmons, D.D. (2002). Development of the inner ear efferent system across vertebrate
879 species. *J Neurobiol* 53(2)**,** 228-250. doi: 10.1002/neu.10130 [doi].
880 Thompson, A.J., Lester, H.A., and Lummis, S.C. (2010). The structural basis of
881 function in Cys-loop receptors. *Q Rev Biophys* 43(4)**,** 449-499. doi:
882 10.1017/s0033583510000168.
883 Tomaselli, G.F., McLaughlin, J.T., Jurman, M.E., Hawrot, E., and Yellen, G. (1991).
884 Mutations affecting agonist sensitivity of the nicotinic acetylcholine receptor.
885 *Biophys J* 60(3)**,** 721-727. doi: 10.1016/s0006-3495(91)82102-6.
886 Verbitsky, M., Rothlin, C., Katz, E., and Elgoyhen, A.B. (2000). Mixed nicotinic-
887 muscarinic properties of the a9 nicotinic cholinergic receptor.
888 *Neuropharmacology* 39**,** 2515-2524.

889 Wehrwein, E.A., Orer, H.S., and Barman, S.M. (2016). Overview of the Anatomy,
890 Physiology, and Pharmacology of the Autonomic Nervous System. *Compr*
891 *Physiol* 6(3)**,** 1239-1278. doi: 10.1002/cphy.c150037.
892 Zhu, B.T. (2005). Mechanistic explanation for the unique pharmacologic properties of
893 receptor partial agonists. *Biomed Pharmacother* 59(3)**,** 76-89. doi:
894 10.1016/j.biopha.2005.01.010.
895 Zouridakis, M., Giastas, P., Zarkadas, E., Chroni-Tzartou, D., Bregestovski, P., and
896 Tzartos, S.J. (2014). Crystal structures of free and antagonist-bound states of
897 human α9 nicotinic receptor extracellular domain. *Nat Struct Mol Biol* 21(11)**,**
898 976-980. doi: 10.1038/nsmb.2900.
899

900

901 **Table 1.** Estimated values of EC_{50} and efficacy for agonists of α9α10 receptors and IC_{50}
902 value for the antagonist nicotine. Values are mean ± S.E.M.. Between brackets, number
903 of oocytes per experiment. R, rat. C, chicken. N.D., not determined.
904

905

	ACh	Choline		Carbachol		DMPP		Nicotine
	EC50 (μM)	EC50 (μM)	Efficacy (%)	EC50 (μM)	Efficacy (%)	EC50 (μM)	Efficacy (%)	IC50 (μM)
Rat α9	12.9 ± 1.1 (5)	188 ± 40 (3)	87.3 ± 6.0 (4)	N.D.	N.D.	N.D.	N.D.	N.D.
Rat α9α10	17.1 ± 3.1 (5)	541 ± 62 (10)	37.5 ± 2.5 (9)	159 ± 31.5 (5)	75.5 ± 5.2 (5)	21.5 ± 4.0 (6)	0.6 ± 0.3 (6)	46.3 ± 12.4 (6)
Chicken α9	12.9 ± 1.4 (5)	280 ± 20 (6)	73.7 ± 5.9 (6)	N.D.	N.D.	N.D.	N.D.	N.D.
Chicken α10	2.2 ± 0.7 (5)	23.2 ± 8.3 (4)	99.4 ± 9.5 (4)	N.D.	N.D.	N.D.	N.D.	N.D.
Chicken α9α10	13.1 ± 2.6 (10)	200 ± 16 (6)	88.0 ± 6.7 (6)	150 ± 15 (6)	89.8 ± 7.0 (6)	9.8 ± 0.5 (5)	32.6 ± 2.9 (5)	39.4 ± 3.4 (6)
Rα9-Cα10	11.6 ± 2.9 (7)	148 ± 12.1 (5)	86.4 ± 2.1 (6)	N.D.	N.D.	N.D.	N.D.	N.D.
Cα9-Rα10	18.2 ± 4.8 (4)	333 ± 66.2 (4)	51.2 ± 6 (5)	N.D.	N.D.	N.D.	N.D.	N.D.
α9α10x	15.6 ± 6.5 (4)	160.2 ± 7.6 (5)	74.3 ± 1.0 (5)	N.D.	N.D.	N.D.	N.D.	N.D.
Rα9-Rα10W55T	37.8 ± 6.2 (8)	N.D.	7.4 ± 1.9 (5)	N.D.	N.D.	N.D.	N.D.	N.D.

906

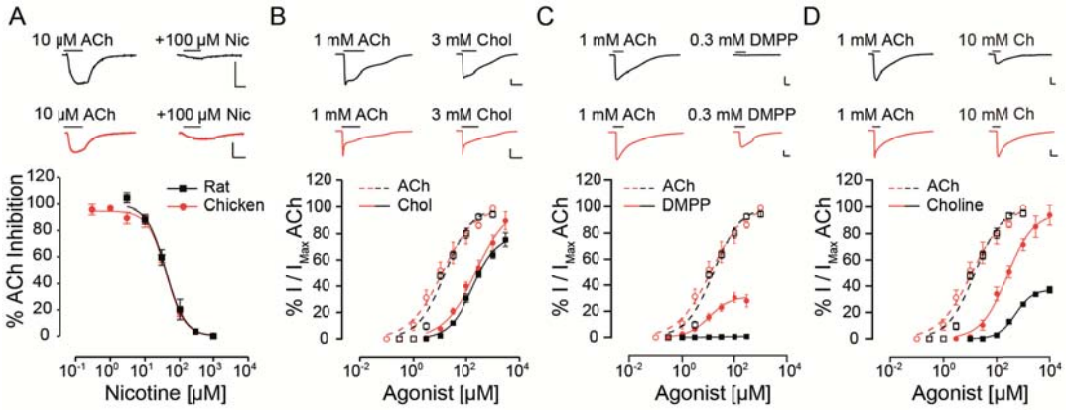

Figure 1. *Responses of rat and chicken recombinant heteromeric α9α10 nAChRs to nicotinic agonists.* A. Top panel: representative traces of responses to 10 μM ACh (left) blocked by co-application of 100 μM nicotine (right) for rat (black traces) and chicken (red traces) α9α10 receptors. Bottom panel: inhibition curves for nicotine for rat and chicken α9α10 receptors. Responses to 10 μM ACh, co-applied with increasing concentrations of nicotine were normalized to the responses to 10 μM ACh alone. Values are mean ± S.E.M. for 6-7 oocytes. B-D. Top panels: representative maximal responses to ACh and carbachol (B), DMPP (C) and choline (D) for rat and chicken α9α10 receptors. Bottom panels: concentration-response curves for ACh (dotted lines) and carbachol (B), DMPP (C) and choline (D) (solid lines) for rat (black) and chicken (red) α9α10 receptors. Values are normalized to the maximal response to ACh obtained in each oocyte. Values are mean ± S.E.M. for 5-9 oocytes.

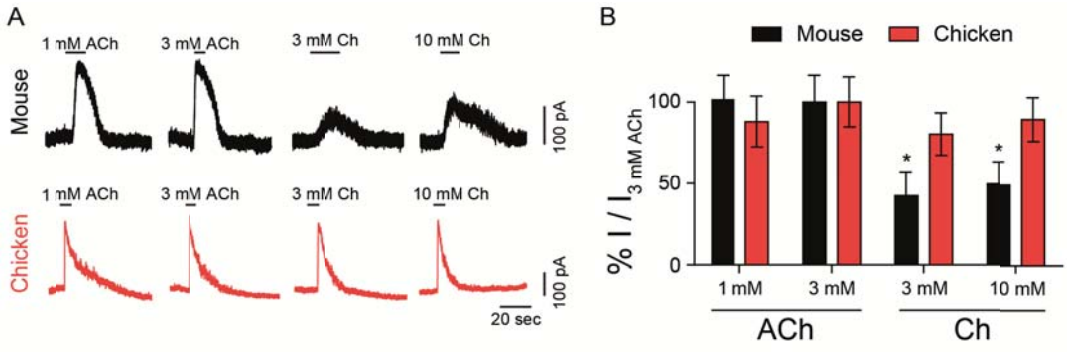

Figure 2. *Responses of hair cells to choline.* A. Representative traces of responses to ACh or choline (Ch) in mouse outer (black, top panel) and chicken short (red, bottom panel) hair cells at a holding potential of -40 mV. B. Percentage of maximum response evoked by ACh or choline normalized to the maximal peak response to 3 mM ACh for mouse and chicken hair cells. Values are mean ± S.E.M. of 6 (rat) and 4 (chicken) experiments per group. (*) Friedman's test, vs 3 mM ACh for each species ($p < 0.05$).

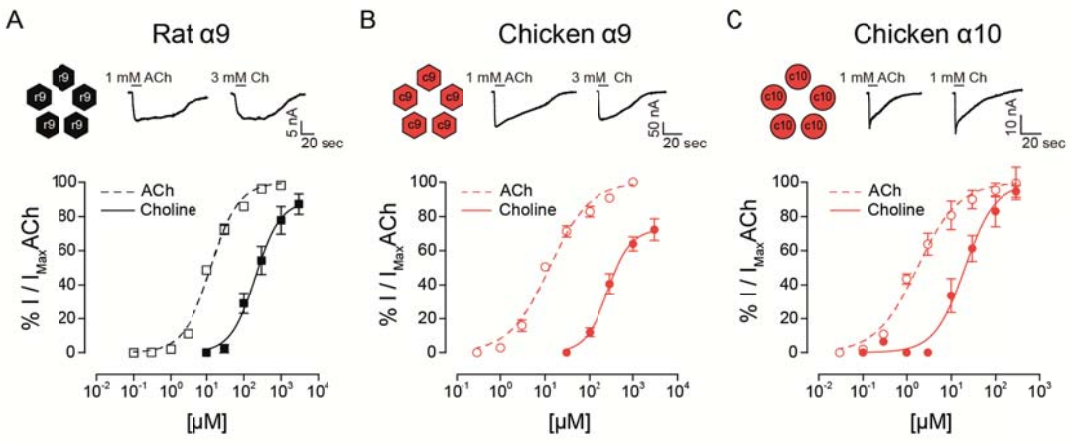

Figure 3. *Responses of rat and chicken homomeric α9 or α10 nAChRs to choline.* Top panels: representative maximal responses to ACh and choline for rat α9 (A), chicken α9 (B) and chicken α10 (C) homomeric receptors. Bottom panels: concentration-response curves for ACh (dotted lines) and choline (solid lines) for rat α9 (A), chicken α9 (B) and chicken α10 (C) homomeric receptors. Values are normalized to the maximal response to ACh obtained in each oocyte. Values are mean ± S.E.M. for 4-6 oocytes.

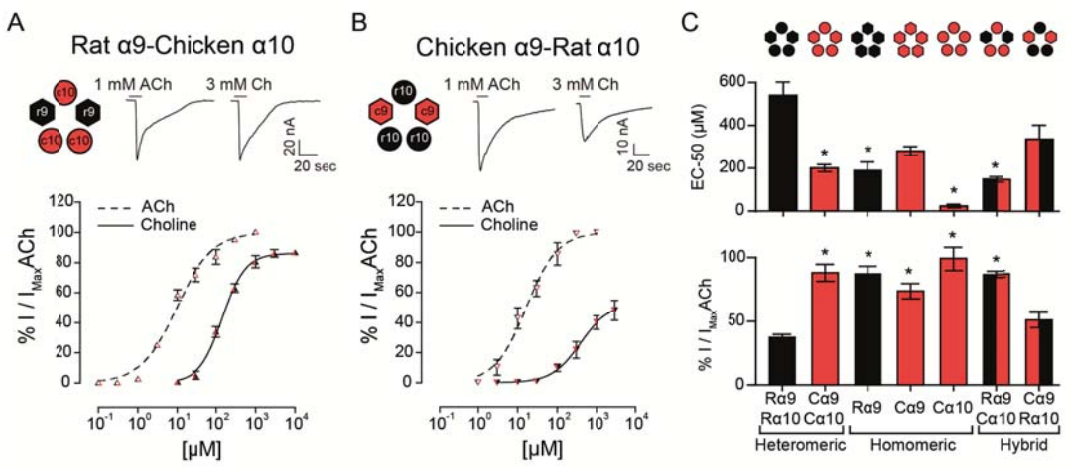

Figure 4. *Responses of rat-chicken hybrid receptors to choline*. A-B. Top panels: representative maximal responses evoked by saturating concentrations of ACh and choline in rat α9 - chicken α10 (A) and chicken α9 - rat α10 (B) hybrid receptors. Bottom panels: concentration-response curves for ACh (dotted lines) and choline (solid lines). Values are normalized to the maximal response to ACh in each oocyte. Values are mean ± S.E.M. of 4-6 oocytes per group. C. EC_{50} values for choline (Top panel) and percentage maximal choline response, normalized to the maximal response elicited by ACh (Bottom panel) for rat and chicken heteromeric α9α10 receptors, rat α9, chicken α9 and chicken α10 homomeric receptors, and rat α9 – chicken α10 and chicken α9 – rat α10 hybrid receptors. (*) Kruskal-Wallis test, vs rat α9α10 receptor ($p<0.05$).

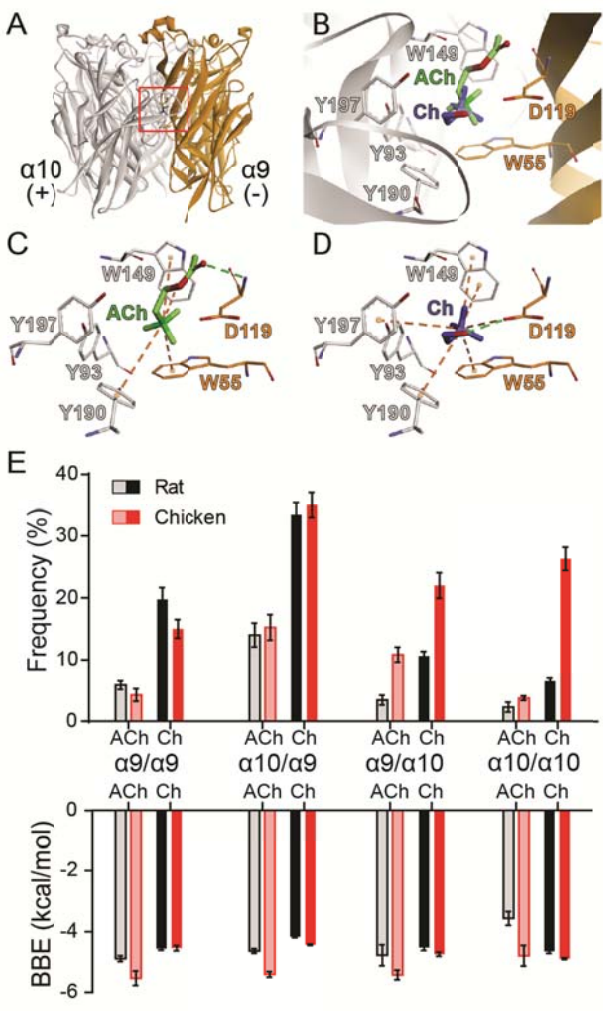

Figure 5. *Docking of ACh and choline into the binding sites of rat and chicken a9a10 receptors.* A. Ribbon structure of the extracellular domain of rat α10 and α9 subunits showing an interface formed by the principal (+) component of the α10 subunit and the complementary (-) component of the α9 subunit. The location of the orthosteric binding site with a bound ACh is highlighted by the red box. B. Detailed view of the binding domain highlighted by the red square in A. ACh (green) and the most frequent orientation of choline (blue) are shown docked into the binding pocket. C-D. Molecular interactions of ACh (C) and choline (D) with residues in the binding site. Cation-π interactions are illustrated by orange dashed lines and H-bonds by green dashed lines. E. Frequency (as percentage) of the most frequent orientation (Top panel) and best binding energy (BBE; Bottom panel) obtained for three separate simulations for ACh and choline docking into each of the binding interfaces, comprised of (principal/complementary components) α9/α9, α10/α9, α9/α10 and α10/α10 rat (black) or chicken (red) subunits. Values are mean ± SEM of at least three different docking simulations for each interface.

971 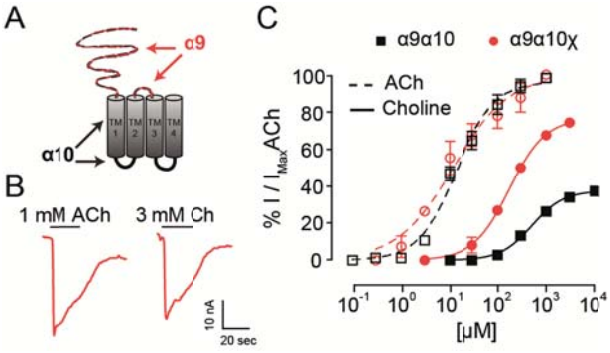

972

980 **Figure 6.** *Responses of rat α9α10$_x$ chimeric receptor to choline.* A. Diagram of an
981 α9α10$_x$ chimeric subunit showing the regions corresponding to the α9 subunit sequence
982 (red) and α10 subunit sequence (black). B. Representative maximal responses to ACh
983 (left) and choline (right) for the α9α10$_x$ chimeric receptor. C. Concentration response-
984 curves for ACh (dotted lines) and choline (solid lines) for α9α10$_x$ chimeric receptors
985 (red circles) and wild-type α9α10 receptors (black squares). Values were normalized to
986 the maximal response to ACh in each oocyte. Values are mean ± S.E.M. of 5-9 oocytes
987 per group.

981

982

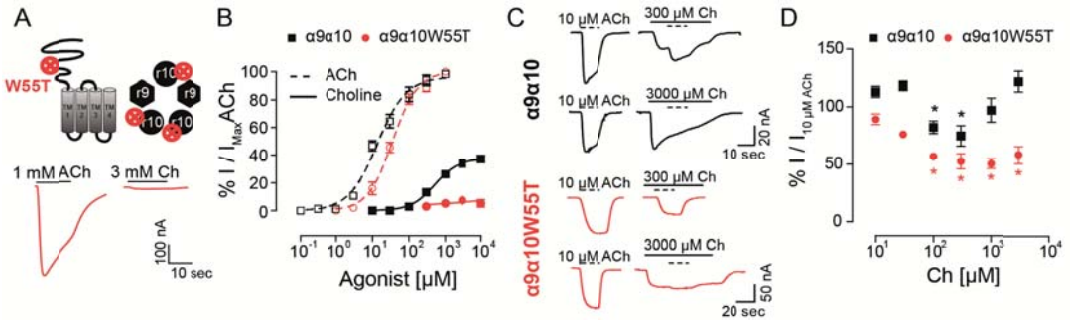

983

996 **Figure 7.** *Responses of the rat α9α10W55T receptor to choline*. A. Diagram of an α10
997 subunit illustrating the position of the W55T mutation, localized to the complementary
998 component of the agonist binding site within the pentameric assembly (Top panel).
999 Representative maximal responses to ACh (left) and choline (right) for the α9α10W55T
900 receptor (Bottom panel). B. Concentration response-curves to ACh (dotted lines) and
901 choline (solid lines) for the α9α10W55T receptor (red circles) and wild-type α9α10
902 receptors (black squares). Values were normalized to the maximal response to ACh in
903 each oocyte. Values are mean ± S.E.M. of 5-9 oocytes per group. C. Representative
904 responses to 10 μM ACh (dotted lines) alone or on top of responses to 300 or 3000 μM
905 choline in oocytes expressing wild-type α9α10 or α9α10W55T receptors. D.
906 Normalized responses to 10 μM ACh obtained in the presence of increasing
907 concentrations of choline for wild-type α9α10 and α9α10W55T receptors. Responses
908 were normalized to responses to10 μM ACh in the absence of choline for each oocyte.

997